A TUTORIAL ON INVERSE ANALYSIS WITH BOUNDARY ELEMENTS

Daniel Lesnic[a] and Liviu Marin[b]
[a]*Department of Applied Mathematics, University of Leeds, Leeds, LS2 9JT, UK*
E-mail: amt5ld@maths.leeds.ac.uk
[b]*School of the Environment, University of Leeds, Leeds, LS2 9JT, UK*
E-mail: liviu@env.leeds.ac.uk

OUTLINE

PART I. FUNDAMENTALS OF THE BOUNDARY ELEMENT METHOD

Aim:
The main aim of Part I is to provide an introduction to a numerical method for solving (linear) partial differential equations (PDEs), namely, the boundary element method (BEM). This method recasts the PDE as a boundary integral equation which is solved numerically.

Advantages:
• It reduces the dimension of the problem by one, i.e. it discretises only the boundary of the solution domain, e.g. curves instead of surfaces in 2D, surfaces instead of volumes in 3D.
• More precisely, it gives the solution of the PDE explicitly, without the need to interpolate onto grid discretisation cells as required by other domain discretisation methods such as the finite-difference method (FDM) or the finite element method (FEM).

Disadvantage:
• Mainly restricted to linear PDEs.

I.1 Partial Differential Equations

Many practical problems in engineering and science are mathematically modelled by partial differential equations of the form

$$L(u(\boldsymbol{x})) = 0, \qquad \boldsymbol{x} \in \Omega, \tag{1}$$

where L is a partial differential operator, such as the Laplace operator $L = \nabla^2 = \Delta = \sum_{i=1}^{d} \frac{\partial^2}{\partial x_i^2}$, $\Omega \subset \mathbb{R}^n$ is the solution domain, d is the dimension of the problem, e.g. $d \in \{1, 2, 3\}$, and u is the solution depending on the position p. Usually, the governing Eqn. (1) has to be solved subject to initial, boundary or other conditions. This mathematical model for a physical phenomenon should be then investigated to establish if it is **well-posed**, i.e. whether there is a unique solution, which in addition is continuously dependent (stable) on the input data, e.g. initial and/or boundary conditions. The stability of the solution is regarded as requiring small perturbations in the input data to cause only small (comparable) errors in the output data. If any of the above three conditions is violated then the problem is called **ill-posed in the**

classical sense of Hadamard, see Hadamard [1]. If the uniqueness of the solution is ensured, but either the existence or stability of the solution is violated then the problem is called **ill-posed in the sense of Tikhonov**, see Tikhonov and Arsenin [2].
In this lecture we will consider only ill-posed problems for which both the existence and uniqueness of solution are ensured, but the stability has to be overcome.

I.2 Integral Equations

The basic idea of the BEM is to multiply Eqn. (1) by an arbitrary function v and integrate "by parts" over Ω. Then the following **general integral equation** is obtained:

$$\begin{aligned} 0 &= \int_{\Omega} v(\boldsymbol{x})\ L(u(\boldsymbol{x}))\ d\Omega(\boldsymbol{x}) \\ &= \int_{\Omega} u(\boldsymbol{x})\ L^*(v(\boldsymbol{x}))\ d\Omega(\boldsymbol{x}) \\ &+ \int_{\partial\Omega} R(u(\boldsymbol{x}), v(\boldsymbol{x}))\ dS(\boldsymbol{x}), \end{aligned} \tag{2}$$

where $\partial\Omega$ is the boundary of Ω, L^* is the adjoint operator of L (analogous to the transpose of a matrix) defined as $< v, L(u) >=< u, L^*(v) >$ for all u, v in some appropriate space of functions, and $R(u, v)$ is a boundary operator which can easily be identified for a particular operator L. For example, when $L = \nabla^2$ then:

$$\begin{aligned} &L^* = \nabla^2, \\ &R(u(\boldsymbol{x}), v(\boldsymbol{x})) = v(\boldsymbol{x})\frac{\partial u(\boldsymbol{x})}{\partial \nu_{\boldsymbol{x}}} - u(\boldsymbol{x})\frac{\partial v(\boldsymbol{x})}{\partial \nu_{\boldsymbol{x}}}, \end{aligned} \tag{3}$$

where $\nu_{\boldsymbol{x}}$ is the outward normal at $\boldsymbol{x} \in \partial\Omega$ and use has been made of Green's identities.
Next, the BEM aims to eliminate the domain integral over Ω in Eqn. (2). In order to do this, we introduce the concept of a fundamental solution for Eqn. (1).

I.3 Fundamental Solutions

A function G is called a **fundamental solution** for Eqn. (1) if

$$L^*(G(\boldsymbol{x}, \boldsymbol{x}')) = -\delta(\boldsymbol{x}, \boldsymbol{x}'), \tag{4}$$

where δ is the Dirac delta distribution which is zero everywhere except at $\boldsymbol{x} = \boldsymbol{x}'$ where it is infinite.
In the case of the Laplace equation $L(u(\boldsymbol{x})) = \nabla^2 u(\boldsymbol{x}) = 0$, using Eqns. (3) and (4) we can obtain the simplest fundamental solution in 2D, see Jaswon and Symm [3],

$$\begin{aligned} G(\boldsymbol{x}, \boldsymbol{x}') &= -\frac{1}{2\pi}\ln|\boldsymbol{x} - \boldsymbol{x}'| \\ &= -\frac{1}{2\pi}\ln\sqrt{(x_1 - x_1')^2 + (x_2 - x_2')^2} \\ &= G(x_1, x_2, x_1', x_2'), \end{aligned} \tag{5}$$

where $\boldsymbol{x}$ and $\boldsymbol{x}'$ have the coordinates (x_1, x_2) and (x_1', x_2'), respectively.

I.4 Boundary Integral Equations

If we take $v = G$ in Eqn. (2) and use Eqn. (5) then we obtain

$$u(\boldsymbol{x}) = \int_{\partial\Omega} R(u(\boldsymbol{x}'), G(\boldsymbol{x}, \boldsymbol{x}'))\ dS(\boldsymbol{x}'),\ \boldsymbol{x} \in \Omega, \tag{6}$$

where use has been made of the fundamental property of the δ function, namely,

$$\int_{\Omega} \delta(\boldsymbol{x}, \boldsymbol{x}')u(\boldsymbol{x}')\ dS(\boldsymbol{x}') = u(\boldsymbol{x}), \quad \boldsymbol{x} \in \Omega. \tag{7}$$

Now based on the limiting process of letting $\boldsymbol{x}$ be a point at the boundary $\partial\Omega$, commonly used in potential theory, see Symm and Pitfield [4], the following **general boundary integral equation** can be obtained:

$$\begin{aligned} &\eta(\boldsymbol{x})u(\boldsymbol{x}) = \int_{\partial\Omega} R(u(\boldsymbol{x}'), G(\boldsymbol{x}, \boldsymbol{x}'))\ dS(\boldsymbol{x}'), \\ &\boldsymbol{x} \in \overline{\Omega} = \Omega \cup \partial\Omega, \end{aligned} \tag{8}$$

where $\eta(\boldsymbol{x}) = 1$ if $\boldsymbol{x} \in \Omega$ and $\eta(\boldsymbol{x}) = \gamma(\boldsymbol{x})/2\pi$ if $\boldsymbol{x} \in \partial\Omega$, where $\gamma(\boldsymbol{x})$ is the angle between the tangents at $\partial\Omega$ at either sides of the point $\boldsymbol{x}$. Note that if $\boldsymbol{x}$ is not a corner then $\gamma(\boldsymbol{x}) = \pi$.
As an example for the Laplace equation, using Eqns. (3), (6) and (8) we obtain the **boundary integral equation**

$$\begin{aligned} &\eta(\boldsymbol{x})u(\boldsymbol{x}) = \\ &\int_{\partial\Omega} \left[G(\boldsymbol{x}, \boldsymbol{x}')\frac{\partial u(\boldsymbol{x}')}{\partial \nu_{\boldsymbol{x}'}} - u(\boldsymbol{x}')\frac{\partial G(\boldsymbol{x}, \boldsymbol{x}')}{\partial \nu_{\boldsymbol{x}'}} \right] dS(\boldsymbol{x}'), \\ &\boldsymbol{x} \in \overline{\Omega}. \end{aligned} \tag{9}$$

I.5 Numerical Discretisation

In practice, boundary integral equations such as (8) or (9) can rarely be solved analytically, therefore some form of numerical approximation is necessary. In order to numerically solve Eqn. (9), we use the following discretisations:
(i) The boundary $\partial\Omega$ is discretised into small **boundary elements**, Γ_j for $j = 1, \ldots, M$, namely, $\partial\Omega = \bigcup_{j=1}^{M} \Gamma_j$, e.g. Γ_j are usually straight

lines if Ω is a 2D domain.
(ii) Over each boundary element Γ_j for $j = 1, \ldots, M$, u and $\partial u/\partial \nu$ are assumed usually to be constant and take their value at the centroid (**node**) $\boldsymbol{x}^j$, e.g. midpoint in 2D, of Γ_j, namely,

$$\begin{aligned} u(\boldsymbol{x}') &\equiv u(\boldsymbol{x}^j) = u_j, \qquad \boldsymbol{x}' \in \Gamma_j, \\ \frac{\partial u(\boldsymbol{x}')}{\partial \nu_{\boldsymbol{x}'}} &\equiv \frac{\partial u(\boldsymbol{x}^j)}{\partial \nu_{\boldsymbol{x}'}} = u'_j, \quad \boldsymbol{x}' \in \Gamma_j. \end{aligned} \tag{10}$$

Then the boundary integral Eqn. (9) can be approximated as:

$$\eta(\boldsymbol{x}) u(\boldsymbol{x}) = \sum_{j=1}^{M} \left[A_j(\boldsymbol{x}) u'_j + B_j(\boldsymbol{x}) u_j \right], \boldsymbol{x} \in \overline{\Omega}, \tag{11}$$

where

$$\begin{aligned} A_j(\boldsymbol{x}) &= \int_{\Gamma_j} G(\boldsymbol{x}, \boldsymbol{x}') \, d\Gamma_j(\boldsymbol{x}'), \\ B_j(\boldsymbol{x}) &= -\int_{\Gamma_j} \frac{\partial G(\boldsymbol{x}, \boldsymbol{x}')}{\partial \nu_{\boldsymbol{x}'}} \, d\Gamma_j(\boldsymbol{x}'). \end{aligned} \tag{12}$$

These integrals can be evaluated exactly for straight-line boundary elements, see e.g. Symm and Pitfield [4].
(iii) Taking $\boldsymbol{x} = \boldsymbol{x}^i$ for $i = 1, \ldots, M$ in Eqn. (11), we obtain a system of linear equations, namely,

$$\sum_{j=1}^{M} \left[A_{ij} u'_j + B_{ij} u_j \right] = 0, i = 1, \ldots, M, \tag{13}$$

where

$$A_{ij} = A_j(\boldsymbol{x}^i), \quad B_{ij} = B_j(\boldsymbol{x}^i) - \eta(\boldsymbol{x}^i)\delta_{ij}, \tag{14}$$

where δ_{ij} is the Kronecker delta symbol which is 0 if $i \neq j$ and 1 if $i = j$.
(iv) Boundary conditions that are associated with the Laplace equation are usually of the Robin type, namely,

$$c_0(\boldsymbol{x}) u(\boldsymbol{x}) + c_1(\boldsymbol{x}) \frac{\partial u(\boldsymbol{x})}{\partial \nu_{\boldsymbol{x}}} = f(\boldsymbol{x}), \quad \boldsymbol{x} \in \partial\Omega, \tag{15}$$

where c_0, c_1 and f are usually prescribed functions. Taking $\boldsymbol{x} = \boldsymbol{x}^i$ for $i = 1, \ldots, M$ in Eqn. (15), we obtain

$$c_0(\boldsymbol{x}^i) u_i + c_1(\boldsymbol{x}^i) u'_i = f(\boldsymbol{x}^i), \quad i = 1, \ldots, M. \tag{16}$$

Now, Eqns. (13) and (16) form a system of $2M$ equations with the unknowns u_i and u'_i for $i = 1, \ldots, M$, which in principle can be solved using a Gaussian elimination procedure. Finally, note that once u_i and u'_i for $i = 1, \ldots, M$ are obtained then the discretised version (11) of the boundary integral Eqn. (9) gives the solution $u(\boldsymbol{x})$ at any point $\boldsymbol{x}$ inside the domain Ω.

PART II. INVERSE PROBLEMS

II.1 Fundamentals of Inverse Problems

In **direct problems**, "the cause determines the effect", such that if we know a matrix $\boldsymbol{C}$ and a vector $\boldsymbol{x}$ then we can easily find the vector

$$\boldsymbol{b} = \boldsymbol{C}\boldsymbol{x}. \tag{17}$$

In **inverse problems**, "the effect determines some cause", such that if we know a matrix $\boldsymbol{C}$ and the vector $\boldsymbol{b}$ then how we can find the vector $\boldsymbol{x}$ from Eqn. (17)?
The main difficulty associated with inverse problems is that in general they are unstable, i.e. the matrix $\boldsymbol{C}$ is usually ill-conditioned such that a straightforward inversion of Eqn. (17) given by $\boldsymbol{x} = \boldsymbol{C}^{-1}\boldsymbol{b}$ produces highly oscillatory and unbounded results. As an example let us now consider the following inverse problem.

II.2 A Cauchy Problem for the Laplace equation

The inverse problem investigated in this section requires finding the data $u(0, y)$ and $-u_x(0, y)$ for the following test boundary value problem:

$$\begin{aligned} &\nabla^2 u(x, y) = 0, \quad (x, y) \in \Omega = (0, 1) \times (0, 1) \\ &u(x, 0) = x^2, \quad u(x, 1) = x^2 - 1, \quad x \in [0, 1] \\ &u(0, y) = 1 - y^2, \quad u(1, y) = 2, \quad y \in [0, 1]. \end{aligned} \tag{18}$$

Mathematically speaking, this problem as proposed by Hadamard in 1923 was beyond Dirichlet's thoughts that the physics may encounter applications in which the data in not uniformly distributed over the boundary as shown above. On the other hand, there are many practical applications in steady heat conduction in which the boundary $x = 0$ is heated to a very high temperature and then the measurements of the temperature $u(0, y)$ with sensors or thermocouples attached to it may become difficult to determine.
It can easily be seen that the Cauchy problem above possesses the solution

$$u(x, y) = x^2 - y^2. \tag{19}$$

Let us now perturb the data $u(1, y)$ on the overspecified boundary $x = 1$ by a small amount $\sin(k\pi y)/k$, where k is a large natural number.

Then the Cauchy problem for the Laplace equation with the perturbed data

$$\overline{u}(1,y) = 1 - y^2 + \sin(k\pi y)/k, \qquad (20)$$

instead of $u(1,y) = 1-y^2$, possesses the solution

$$\overline{u}(x,y) = x^2 - y^2 + \sin(k\pi y)\cosh(k\pi(1-x))/k, \qquad (21)$$

which becomes unbounded for $0 \leq x < 1$ as $k \to \infty$. From this example it can be seen that as $k \to \infty$, whilst the difference between the input data $\overline{u}(1,y)$ and $u(1,y)$ becomes vanishingly small, the difference between the required output data $\overline{u}(0,y)$ and $u(0,y)$ becomes infinitely large with high and unbounded oscillations occurring. Hence the solution is unstable and, consequently, the Cauchy problem for the Laplace equation is ill-posed. Therefore, some sort of regularization is necessary in order to overcome this instability.

II.3 Regularization Methods

The Cauchy problem for the Laplace equation setup in Section II.2, has been solved numerically in Zeb *et al.* [5] using the BEM described in Part I, as a direct solution procedure, for obtaining the generically written system of Eqns. (17). However, instead of solving the ill-conditioned system of Eqns. (17) by an unstable inversion $\boldsymbol{x} = \boldsymbol{C}^{-1}\boldsymbol{b}$, we use a stable regularization method given by the minimization of the Tikhonov functional, see Twomey [6],

$$T_\lambda(\boldsymbol{x}) = (\boldsymbol{C}\boldsymbol{x} - \boldsymbol{b})^T(\boldsymbol{C}\boldsymbol{x} - \boldsymbol{b}) + \lambda(\boldsymbol{R}\boldsymbol{x})^T(\boldsymbol{R}\boldsymbol{x}), \qquad (22)$$

where

$$\boldsymbol{R}^T\boldsymbol{R} = \begin{bmatrix} 1 & 0 & . \\ 0 & 1 & . \\ . & . & . \end{bmatrix} \qquad (23)$$

(zeroth-order regularization)

$$\boldsymbol{R}^T\boldsymbol{R} = \begin{bmatrix} 1 & -1 & 0 & 0 & . \\ -1 & 2 & -1 & 0 & . \\ 0 & -1 & 2 & -1 & . \\ . & . & . & . & . \end{bmatrix} \qquad (24)$$

(first-order regularization)

$$\boldsymbol{R}^T\boldsymbol{R} = \begin{bmatrix} 1 & -2 & 1 & 0 & 0 & . & . & . \\ -2 & 5 & -4 & 1 & 0 & . & . & . \\ 1 & -4 & 6 & -4 & 1 & 0 & . & . \\ 0 & 1 & -4 & 6 & -4 & 1 & 0 & . \\ . & . & . & . & . & . & . & . \end{bmatrix} \qquad (25)$$

(second-order regularization)

and $\lambda > 0$ is a regularization parameter (Lagrange multiplier) whose choice can be based on:

(i) **The Discrepancy Principle**, see Morozov [7];
(ii) **The Cross-Validation Principle**, see Wahba [8];
(iii) **The L-curve Principle**, see Hansen [9].

Corresponding to Eqns. (23) – (25) via Eqn. (22), the regularization method imposes continuity, i.e. class $\mathcal{C}^0$, first-order smoothness, i.e. class $\mathcal{C}^1$, or second-order smoothness, i.e. class $\mathcal{C}^2$, for the solution $\boldsymbol{x}$.
Minimising the Tikhonov functional T_λ we obtain the solution $\boldsymbol{x}$ depending on λ, namely,

$$\boldsymbol{x}_\lambda = \left(\boldsymbol{C}^T\boldsymbol{C} + \lambda\boldsymbol{R}^T\boldsymbol{R}\right)^{-1}\boldsymbol{C}^T\boldsymbol{b}. \qquad (26)$$

PART III. AN APPLICATION TO ELASTICITY

In this section we give a practical application of an inverse problem in elasticity solved using the BEM, see Marin and Lesnic [10] for more details.

III.1 Mathematical Formulation

We consider an isotropic linear elastic material which occupies an open bounded domain $\Omega \subset \mathbb{R}^2$ and assume that the boundary $\Gamma \equiv \partial\Omega$ is smooth in the sense of Liapunov such that Green's formula is applicable, see Kellogg [11]. In the absence of body forces, the equilibrium equations written with respect to the displacement vector $\boldsymbol{u}(\boldsymbol{x})$ may be recast in the form of the Lamé equations, see Saada [12], namely

$$G\frac{\partial^2 u_i(\boldsymbol{x})}{\partial x_j \partial x_j} + \frac{G}{1-2\nu}\frac{\partial^2 u_j(\boldsymbol{x})}{\partial x_i \partial x_j} = 0, \ \boldsymbol{x} \in \Omega, \qquad (27)$$

where the constants G and ν are the shear modulus and the Poisson ratio, respectively.
We now let $\boldsymbol{n}(\boldsymbol{x})$ be the outward normal vector at Γ and $\boldsymbol{t}(\boldsymbol{x})$ be the traction vector at a point $\boldsymbol{x} \in \Gamma$ whose components are defined by

$$t_i(\boldsymbol{x}) = \sigma_{ij}(\boldsymbol{x})\, n_j(\boldsymbol{x}), \quad \boldsymbol{x} \in \Gamma, \qquad (28)$$

where $\sigma_{ij}(\boldsymbol{x})$ is the stress tensor. In the direct problem formulation, the knowledge of the material constants G and ν, the location, shape and size of the entire boundary Γ, and the traction and/or displacement vectors on the boundary Γ gives the corresponding Neumann, Dirichlet,

or mixed boundary problems which enable one to determine the displacement vector $\boldsymbol{u}(\boldsymbol{x})$ in the domain Ω. A different and more interesting inverse situation occurs when a part of the boundary Γ is unknown and some additional information is supplied on the remaining part of the boundary. More specifically, we analyse the following problem:

Find the boundary $\Gamma_2 \subset \Gamma$ such that the displacement vector $\boldsymbol{u}$ satisfies the Lamé equations (27)*, either Dirichlet or Neumann boundary conditions are given on Γ_2, with the mention that the traction field on Γ_2 is assumed to be conservative, and the displacement and the traction vectors, i.e. Cauchy data, are known on the remaining part $\Gamma_1 = \Gamma \setminus \Gamma_2$ of the boundary, namely*

$$\boldsymbol{u}(\boldsymbol{x}) = \widetilde{\boldsymbol{u}}(\boldsymbol{x}) \text{ and } \boldsymbol{t}(\boldsymbol{x}) = \widetilde{\boldsymbol{t}}(\boldsymbol{x}), \ \boldsymbol{x} \in \Gamma_1, \quad (29)$$

$$\boldsymbol{u}(\boldsymbol{x}) = \widetilde{\boldsymbol{u}}(\boldsymbol{x}) \text{ or } \boldsymbol{t}(\boldsymbol{x}) = \widetilde{\boldsymbol{t}}(\boldsymbol{x}), \ \boldsymbol{x} \in \Gamma_2. \quad (30)$$

III.2 Boundary Element Method

The Lamé system (27) can be formulated in integral form with the aid of the Second Theorem of Betti, see Saada [12], namely

$$\begin{aligned} &C_{ij}(\boldsymbol{x})u_j(\boldsymbol{x}) + \fint_\Gamma T_{ij}(\boldsymbol{y},\boldsymbol{x})u_j(\boldsymbol{y})\ d\Gamma(\boldsymbol{y}) \\ &= \int_\Gamma U_{ij}(\boldsymbol{y},\boldsymbol{x})t_j(\boldsymbol{y})\ d\Gamma(\boldsymbol{y}), \quad \boldsymbol{x} \in \overline{\Omega}, \end{aligned} \quad (31)$$

where the first integral is taken in the sense of the Cauchy principal value, $C_{ij}(\boldsymbol{x}) = 1$ for $\boldsymbol{x} \in \Omega$ and $C_{ij}(\boldsymbol{x}) = 1/2$ for $\boldsymbol{x} \in \Gamma$ (smooth), and U_{ij} and T_{ij} are the fundamental displacements and tractions, respectively, for the 2D isotropic linear elasticity, see e.g. Brebbia *et al.* [13].

Since the integral equation (31) cannot, in general, be solved analytically, the boundary Γ of the solution domain Ω is discretised in an anticlockwise direction into N continuous linear boundary elements Γ_K, $K = 1, \ldots, N$, having the endpoints $\boldsymbol{x}^K = \left(x_1^K, x_2^K\right)$ and $\boldsymbol{x}^{K+1} = \left(x_1^{K+1}, x_2^{K+1}\right)$, $K = 1, \ldots, N$, where $\boldsymbol{x}^{N+1} \equiv \boldsymbol{x}^0$. On applying the continuous linear BEM approximation in which the unknowns u_j and t_j are assumed linear over each boundary element Γ_K, we obtain

$$\begin{aligned} &u_j(\boldsymbol{y}) \\ &= u_j(\boldsymbol{x}^K)\frac{|\boldsymbol{x}^{K+1} - \boldsymbol{y}|}{|\boldsymbol{x}^{K+1} - \boldsymbol{x}^K|} + u_j(\boldsymbol{x}^K)\frac{|\boldsymbol{y} - \boldsymbol{x}^K|}{|\boldsymbol{x}^{K+1} - \boldsymbol{x}^K|} \\ &\equiv u_j^K \frac{|\boldsymbol{x}^{K+1} - \boldsymbol{y}|}{|\boldsymbol{x}^{K+1} - \boldsymbol{x}^K|} + u_j^{K+1}\frac{|\boldsymbol{y} - \boldsymbol{x}^K|}{|\boldsymbol{x}^{K+1} - \boldsymbol{x}^K|}, \\ &\boldsymbol{y} \in \Gamma_K \end{aligned} \quad (32)$$

$$\begin{aligned} &t_j(\boldsymbol{y}) \\ &= t_j(\boldsymbol{x}^K)\frac{|\boldsymbol{x}^{K+1} - \boldsymbol{y}|}{|\boldsymbol{x}^{K+1} - \boldsymbol{x}^K|} + t_j(\boldsymbol{x}^K)\frac{|\boldsymbol{y} - \boldsymbol{x}^K|}{|\boldsymbol{x}^{K+1} - \boldsymbol{x}^K|} \\ &\equiv t_j^K \frac{|\boldsymbol{x}^{K+1} - \boldsymbol{y}|}{|\boldsymbol{x}^{K+1} - \boldsymbol{x}^K|} + t_j^{K+1}\frac{|\boldsymbol{y} - \boldsymbol{x}^K|}{|\boldsymbol{x}^{K+1} - \boldsymbol{x}^K|}, \\ &\boldsymbol{y} \in \Gamma_K. \end{aligned} \quad (33)$$

Thus relation (31) recasts as

$$\begin{aligned} &\sum_{j=1}^{2} C_{ij}(\boldsymbol{x})u_j(\boldsymbol{x}) + \sum_{K=1}^{N}\sum_{j=1}^{2} A_{ij}^K(\boldsymbol{x})u_j^K \\ &= \sum_{K=1}^{N}\sum_{j=1}^{2} B_{ij}^K(\boldsymbol{x})t_j^K, \\ &i = 1,2, \quad L = 1, \ldots, N, \quad \boldsymbol{x} \in \overline{\Omega}. \end{aligned} \quad (34)$$

Here N_1 is the number of boundary elements on Γ_1, N_2 is the number of boundary elements on Γ_2, $N = N_1 + N_2$, and the functions $A_{ij}^K(\boldsymbol{x})$ and $B_{ij}^K(\boldsymbol{x})$, $i, j = 1, 2$, $K = 1, \ldots, N$, depend on the geometry of the boundary Γ and may be evaluated analytically, see Marin *et al.* [14]. Collocating equation (34) at each boundary node $\boldsymbol{x}^L$, $L = 1, \ldots, N$, we arrive at the system of equations

$$\begin{aligned} &\sum_{K=1}^{N}\sum_{j=1}^{2}\left(A_{ij}^{KL}u_j^K - B_{ij}^{KL}t_j^K\right) = 0, \\ &i = 1,2, \quad L = 1, \ldots, N, \end{aligned} \quad (35)$$

where A_{ij}^{KL} and B_{ij}^{KL}, $i, j = 1, 2$ and $K, L = 1, \ldots, N$, are given by

$$\begin{aligned} A_{ij}^{KL} &= A_{ij}^K(\boldsymbol{x}^L) + C_{ij}(\boldsymbol{x}^L), \\ B_{ij}^{KL} &= B_{ij}^K(\boldsymbol{x}^L). \end{aligned} \quad (36)$$

III.3 Description of the Algorithm

It should be noted that the unknown boundary Γ_2 is completely determined by the vector $\boldsymbol{X} = \left(\boldsymbol{x}^{N_1+2}, \ldots, \boldsymbol{x}^N\right)^T \in \mathbb{R}^{2(N_2-1)}$, i.e. $\Gamma_2 = \Gamma_2(\boldsymbol{X})$. If we consider the discretised BEM system (35) recast as the solution of a direct problem with boundary conditions (29_2) and (30_1),

namely

$$\begin{aligned}&\sum_{K=1}^{N_1+1}\sum_{j=1}^{2}A_{ij}^{KL}u_j^K-\sum_{K=N_1+2}^{N}\sum_{j=1}^{2}B_{ij}^{KL}t_j^K\\&=\sum_{K=1}^{N_1+1}\sum_{j=1}^{2}B_{ij}^{KL}\widetilde{t}_j^K-\sum_{K=N_1+2}^{N}\sum_{j=1}^{2}A_{ij}^{KL}\widetilde{u}_j^K,\\&i=1,2,\quad L=1,\ldots,N,\end{aligned}\tag{37}$$

then the calculated displacements u_j^K, $j=1,2$ and $K=1,\ldots,(N_1+1)$, on the known boundary Γ_1 and tractions t_j^K, $j=1,2$ and $K=(N_1+2),\ldots,N$, on the unknown boundary Γ_2 are functions of the unknown parameters given by the vector $\boldsymbol{X}$, i.e.

$$u_j^K=u_j^K(\boldsymbol{X}),\ j=1,2,\ K=1,\ldots,(N_1+1),\tag{38}$$

$$t_j^K=t_j^K(\boldsymbol{X}),\ j=1,2,\ K=(N_1+2),\ldots,N.\tag{39}$$

The numerical scheme proposed in this study is based on the minimisation of the Tikhonov functional

$$\begin{aligned}&\mathcal{F}_\lambda(\cdot):\mathbb{R}^{2(N_2-1)}\longrightarrow[0,\infty)\\&\mathcal{F}_\lambda(\boldsymbol{X})=\tfrac{1}{2}\|\boldsymbol{u}^{(\mathrm{num})}(\boldsymbol{X})|_{\Gamma_1}-\widetilde{\boldsymbol{u}}^{\varepsilon}|_{\Gamma_1}\|_2^2\\&+\lambda\sum_{K=N_1+1}^{N}\|\boldsymbol{x}^{K+1}-\boldsymbol{x}^K\|_2^2\end{aligned}\tag{40}$$

with respect to the vector

$$\boldsymbol{X}=\left(\boldsymbol{x}^{N_1+2},\ldots,\boldsymbol{x}^N\right)^T\in\mathbb{R}^{2(N_2-1)},$$

provided that an initial guess $\boldsymbol{X}^{(0)}\in\mathbb{R}^{2(N_2-1)}$ is given, where $\lambda>0$ is a regularization parameter to be prescribed,

$\boldsymbol{u}^{(\mathrm{num})}(\boldsymbol{X})|_{\Gamma_1}=\left(\boldsymbol{u}^1(\boldsymbol{X}),\ldots,\boldsymbol{u}^{N_1+1}(\boldsymbol{X})\right)^T$,

$\boldsymbol{u}^K(\boldsymbol{X})=\left(u_1^K(\boldsymbol{X}),u_2^K(\boldsymbol{X})\right)$, $K=1,\ldots,(N_1+1)$,

is the vector containing the calculated values of the displacement vector on Γ_1 and $\widetilde{\boldsymbol{u}}^{\varepsilon}|_{\Gamma_1}$ represents a noisy measurement data for the exact data $\widetilde{\boldsymbol{u}}|_{\Gamma_1}$.

Numerically, the objective functional (40) is minimised using the NAG subroutine E04UPF, which is designed to minimise an arbitrary smooth sum of squares subject to constraints. This may include simple bounds on the variables, linear constraints and smooth nonlinear constraints. Each iteration of the subroutine includes the following: (a) the solution of a quadratic programming subproblem; (b) a line search with an augmented Lagrangian function; and (c) a quasi-Newton update of the approximate Hessian of the Lagrangian function, for more details see Gill *et al.* [15]. The gradient of the objective functional (40) has been calculated using forward finite differences with a step of 10^{-3} which was found to be sufficiently small that a further decrease in this value does not affect significantly the accuracy of the numerical results.

III.4 Numerical Results and Discussion

In this section, we consider the case when the unknown boundary Γ_2 is the graph of an unknown function $f:[-R,R]\longrightarrow\mathbb{R}$, $R>0$, taking the x_1-axis to pass through the endpoints $f(-R)=f(R)=0$ and fixing the origin at $x_1=0$. Therefore, the endpoints of the boundary elements Γ_K on Γ_2 will have the known equally-spaced x_1-coordinates $x_1^K=R(2K-2-N-N_1)/(N-N_1)$ for $K=(N_1+1),\ldots,(N+1)$. Furthermore, since $f(-R)=f(R)=0$, the functional (40) will depend on only (N_2-1) unknowns, namely $x_2^{N_1+2},\ldots,x_2^N$, where $x_2^K=f(x_1^K)$ for $K=(N_1+2),\ldots,N$. Consequently, the functional (40) has the following form:

$$\begin{aligned}&\mathcal{F}_\lambda(\cdot):\mathbb{R}^{N_2-1}\longrightarrow[0,\infty)\\&\mathcal{F}_\lambda(\boldsymbol{X})\\&=\tfrac{1}{2}\|\boldsymbol{u}^{(\mathrm{num})}(\boldsymbol{X})|_{\Gamma_1}-\widetilde{\boldsymbol{u}}^{\varepsilon}|_{\Gamma_1}\|_2^2+\lambda\|\boldsymbol{X}'\|_2^2\\&=\tfrac{1}{2}\sum_{K=1}^{N_1+1}\sum_{j=1}^{2}\left(u_j^K(\boldsymbol{X})-(\widetilde{u}_j^K)^{\varepsilon}\right)^2+\lambda\Big[\left(x_2^{N_1+2}\right)^2\\&+\sum_{K=N_1+2}^{N-1}\left(x_2^{K+1}-x_2^K\right)^2+\left(x_2^N\right)^2\Big]\end{aligned}\tag{41}$$

where we have stopped penalising the x_1- coordinates in the norms $\|\boldsymbol{x}^{K+1}-\boldsymbol{x}^K\|_2^2$ since they are known. It should be noted that the zeroth-order regularization procedure based on penalising the norm of the solution $\boldsymbol{X}$, rather than its derivative $\boldsymbol{X}'$, did not produce sufficiently accurate and stable numerical results and this conclusion is in accordance with the results obtained by Peneau *et al.* [16] and Lesnic *et al.* [17] who have solved a similar problem for the Laplace equation. Therefore, the assumption of smoothness of the numerical solution for Γ_2, as given by the first-order Tikhonov functional (41), is essential in order to obtain an accurate and stable numerical solution. Alternatively, instead of employing the functional (41), one may parameterise the unknown boundary Γ_2 with various approximating functions and the problem reduces to determining the coefficients of the approximation, see Birginie *et al.* [18].

We solve the inverse problem in the following 2D smooth geometry for an isotropic linear elastic medium characterised by the material constants

$G = 3.35 \times 10^{10}$ N/m^2 and $\nu = 0.34$ corresponding to a copper alloy:

Example. We consider the domain Ω which is bounded by the following curves

$$\Gamma_1 = \left\{ (x_1, x_2) \;\middle|\; \begin{array}{l} x_1^2 + x_2^2 = R^2 \\ -R \le x_1 \le R,\ 0 < x_2 \end{array} \right\} \tag{42}$$

$$\begin{aligned} \Gamma_2 &= \Gamma \setminus \Gamma_1 \\ &= \left\{ (x_1, x_2) \;\middle|\; \begin{array}{l} (x_1 + 3R/4)^2 + x_2^2 = (R/4)^2 \\ -R < x_1 < -R/2,\ x_2 < 0 \end{array} \right\} \\ &\cup \left\{ (x_1, x_2) \;\middle|\; \begin{array}{l} x_1^2 + x_2^2 = (R/2)^2 \\ -R/2 \le x_1 \le R/2,\ 0 < x_2 \end{array} \right\} \\ &\cup \left\{ (x_1, x_2) \;\middle|\; \begin{array}{l} (x_1 - 3R/4)^2 + x_2^2 = (R/4)^2 \\ R/2 < x_1 < R,\ x_2 < 0 \end{array} \right\} \end{aligned} \tag{43}$$

such that the following tractions act on its boundary Γ

$$\begin{aligned} t_1^{(\mathrm{an})}(\boldsymbol{x}) &= \left\{ \begin{array}{ll} \sigma_0, & \boldsymbol{x} \in \Gamma_1 \\ 0, & \boldsymbol{x} \in \Gamma_2 \end{array} \right. , \\ t_2^{(\mathrm{an})}(\boldsymbol{x}) &= \ 0, \quad \boldsymbol{x} \in \Gamma_1 \cup \Gamma_2, \end{aligned} \tag{44}$$

where $\sigma_0 = 1.0 \times 10^{10}$ N/m^2. It should be noted that the analytical expressions for the displacement vector $\boldsymbol{u}^{(\mathrm{an})}(\boldsymbol{x})$ corresponding to this example are not available. However, these can be obtained by solving the following Neumann problem

$$\left\{ \begin{array}{l} G \dfrac{\partial^2 u_i^{(\mathrm{an})}(\boldsymbol{x})}{\partial x_j \partial x_j} + \dfrac{G}{1-2\nu} \dfrac{\partial^2 u_j^{(\mathrm{an})}(\boldsymbol{x})}{\partial x_i \partial x_j} = 0,\ \boldsymbol{x} \in \Omega \\ t_1^{(\mathrm{an})}(\boldsymbol{x}) = \sigma_0, \quad t_2^{(\mathrm{an})}(\boldsymbol{x}) = 0,\ \boldsymbol{x} \in \Gamma_1 \\ t_1^{(\mathrm{an})}(\boldsymbol{x}) = t_2^{(\mathrm{an})}(\boldsymbol{x}) = 0,\ \boldsymbol{x} \in \Gamma_2 \end{array} \right. \tag{45}$$

and eliminating the rigid body displacements according to the formulae

$$\int_\Omega \boldsymbol{u}(\boldsymbol{x})\ d\Omega(\boldsymbol{x}) = 0, \ \int_\Omega \boldsymbol{u}(\boldsymbol{x}) \times \boldsymbol{x}\ d\Omega(\boldsymbol{x}) = 0. \tag{46}$$

In a similar manner, we may create boundary data which is exempt from any numerical noise even when analytical expressions for the displacement and the traction vectors are available and, in what follows, they will be referred to as "exact data". Hence the inverse problem under investigation is given by equations (27), (29) and (30_1) in which the input traction data $\widetilde{\boldsymbol{t}}|_{\Gamma_1} = \boldsymbol{t}^{(\mathrm{an})}|_{\Gamma_1}$ is given by relation (44) and the input displacement data $\widetilde{\boldsymbol{u}}|_\Gamma = \boldsymbol{u}^{(\mathrm{an})}|_\Gamma$ is given by solving numerically the Neumann problem (45) with the traction boundary condition given by relation (44).

The numerical results presented in this section have been obtained using a discretisation of the boundaries Γ, Γ_1 and Γ_2 with $N_1 = N_2 = 20$ boundary elements, such that $N = N_1 + N_2 = 40$ boundary elements. These values were found to be sufficiently large such that any further refinement of the mesh size did not significantly improve the accuracy of the results.

Exact data is seldom available in practice since measurement errors always include noise in the prescribed boundary conditions. In order to investigate the stability of the numerical method proposed, the boundary data $\widetilde{\boldsymbol{u}}|_{\Gamma_1}$ has been perturbed as

$$\begin{aligned} \widetilde{u}_i^{\varepsilon}|_{\Gamma_1} &= \widetilde{u}_i|_{\Gamma_1} + \delta\widetilde{u}_i, \\ \delta\widetilde{u}_i &= \mathrm{G05DDF}(0, \sigma_i), \\ \sigma_i &= \max_{\Gamma_1} |\widetilde{u}_i| \frac{p}{100}, \end{aligned} \tag{47}$$

where $\delta\widetilde{u}_i$ is a Gaussian random variable with mean zero and standard deviation σ_i, generated by the NAG subroutine G05DDF, and $p \in \{1, 2, 3\}$ is the percentage of additive noise included into the input data $\widetilde{\boldsymbol{u}}|_{\Gamma_1}$ in order to simulate the inherent measurement errors.

In the inverse analysis of retrieving the unknown boundary Γ_2, the initial guess $\boldsymbol{X}^{(0)} \in \mathbb{R}^{2(N_2-1)}$ for the minimisation of the objective functional (41) has been taken, for simplicity, to be zero. In order to study the convergence of the numerical method employed, we consider the accuracy error defined by

$$E_X = ||\boldsymbol{X}_\lambda - \boldsymbol{X}^{(\mathrm{ex})}||_2, \tag{48}$$

where $\boldsymbol{X}^{(\mathrm{ex})}$ and $\boldsymbol{X}_\lambda$ are vectors containing the exact and the numerical values corresponding to a specified value of the regularization parameter λ for the coordinates of the unknown boundary Γ_2, respectively. Figure 1 presents the accuracy error E_X defined by relation (48), as a function of the regularization parameter λ obtained for various levels of noise added into the input displacement data $\widetilde{\boldsymbol{u}}|_{\Gamma_1}$. From this figure it can be seen that for the error E_X to attain its minimum requires the optimal value λ_{opt} of the regularization parameter λ to be chosen when using the Tikhonov regularization method and this will be discussed later. Moreover, the minimum value of E_X decreases as the noise added into the input data decreases.

The error which measures the least-squares gap defined by

$$E_u = ||\boldsymbol{u}^{(\mathrm{num})}(\boldsymbol{X}_\lambda)|_{\Gamma_1} - \boldsymbol{u}^{(\mathrm{an})}|_{\Gamma_1}||_2, \tag{49}$$

where $\boldsymbol{u}^{(\mathrm{an})}|_{\Gamma_1}$ and $\boldsymbol{u}^{(\mathrm{num})}(\boldsymbol{X}_\lambda)|_{\Gamma_1}$ are vectors containing the analytical and the numerical values corresponding to a specified value of the

regularization parameter λ, respectively, for the components of the displacement vector at the nodes on the known boundary Γ_1, has a qualitative behaviour similar to that of the error E_X. Figure 2 shows the error E_u as a function of the regularization parameter λ obtained for various amounts of noise added into the input displacement data $\widetilde{\boldsymbol{u}}|_{\Gamma_1}$. From this figure it can be seen that the error E_u decreases as the level of noise added into the input displacement data decreases for all the values of the regularization parameter λ. Furthermore, for all the amounts of noise added into the displacement data $\widetilde{\boldsymbol{u}}|_{\Gamma_1}$, the error E_u decreases down to a constant value as the regularization parameter λ continues to decrease. By comparing Figures 1 and 2, it can be seen, for various levels of noise, that the corner corresponding to the beginning of the constant region in the error E_u occurs at about the same value of the regularization parameter λ where the minimum in the accuracy error E_X is attained.

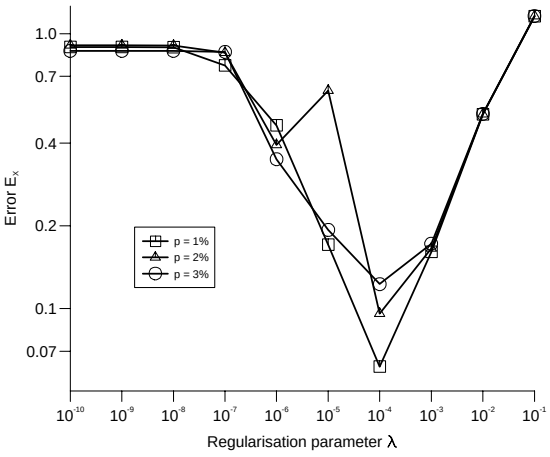

Figure 1: The error $E_X = ||\boldsymbol{X}_\lambda - \boldsymbol{X}^{(\mathrm{ex})}||_2$, as a function of the regularisation parameter λ.

In the functional (41), the choice of the optimal regularization parameter $\lambda = \lambda_{opt}$ is essential in order to achieve the stability on the numerical solution. In this study, we have used an L-curve type criterion, see Hansen [9], which plots on a log-log scale the least-squares gap, i.e. the error $E_u = ||\boldsymbol{u}^{(\mathrm{num})}(\boldsymbol{X})|_{\Gamma_1} - \boldsymbol{u}^{(\mathrm{an})}|_{\Gamma_1}||_2$, versus the norm of the derivative of the solution, $||\boldsymbol{X}'||_2$, for various values of the regularization parameter λ. In Figure 3 we present the L-curve plots obtained for various levels of noise added into the input displacement data $\widetilde{\boldsymbol{u}}|_{\Gamma_1}$, namely $p \in \{1, 2, 3\}$. The optimal values, λ_{opt},

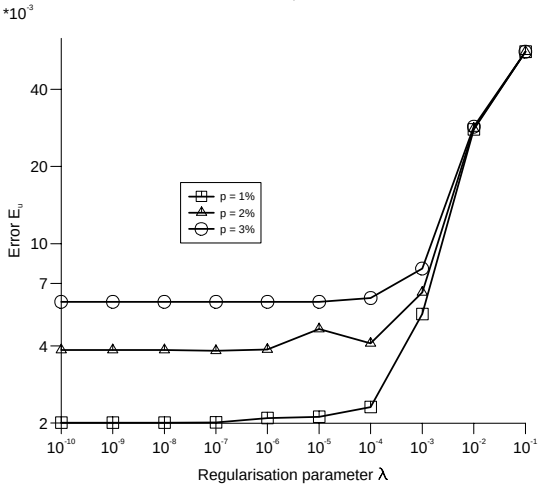

Figure 2: The error $E_u = ||\boldsymbol{u}^{(\mathrm{num})}(\boldsymbol{X}_\lambda)|_{\Gamma_1} - \boldsymbol{u}^{(\mathrm{an})}|_{\Gamma_1}||_2$, as a function of the regularisation parameter λ.

of the regularization parameter, λ, are chosen at the corners of these curves in order to balance the under-smooth regions, i.e. λ too small, and the over-smooth regions, i.e. λ too large. A more systematic way to find this corner is to determine the maximum point of the curvature of the L-curve with respect to the regularization parameter, $\lambda > 0$, for more details on this method we refer the reader to Hansen [9, 19]. Alternatively to this heuristical method, one may use other more rigorous criteria, such as the discrepancy principle, see Morozov [7], or the generalised cross-validation principle, see Wahba [8]. However, Figure 3 illustrates clearly the L-shaped curves and therefore the L-curve criterion is applicable. The optimal values, λ_{opt}, of the regularization parameter, λ, obtained for the example considered in this study are showed in this figure for various levels of noise added into the input displacement data $\widetilde{\boldsymbol{u}}|_{\Gamma_1}$.

Figure 4 illustrates the initial guess, the exact and the numerical values for the unknown boundary Γ_2 obtained using the optimal regularization parameter $\lambda = \lambda_{opt}$ chosen according to the L-curve criterion and various levels of noise added into the input displacement data $\widetilde{\boldsymbol{u}}|_{\Gamma_1}$, namely $p \in \{1, 2, 3\}$. From Figure 4 it can be seen that for the example considered the numerical solutions are stable and consistent with the amount of noise p added into the input data $\widetilde{\boldsymbol{u}}|_{\Gamma_1}$. Moreover, they converge to their corresponding exact targets Γ_2, given by equation (43), as the amount of noise p decreases, i.e. as the data errors tend to zero. Thus, the numerical solution

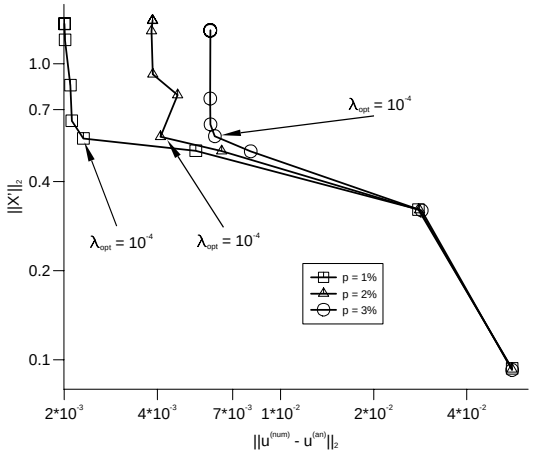

Figure 3: The L-curves obtained with various levels of noise added into the displacement data $\boldsymbol{u}^{(\mathrm{an})}|_{\Gamma_1}$.

is convergent to the exact solution.

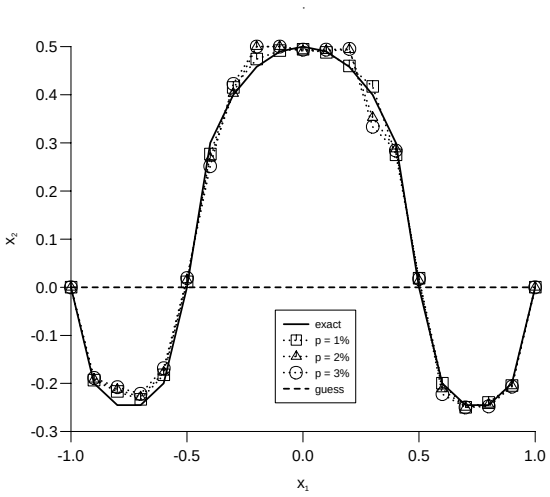

Figure 4: The exact (——), the initial guess (– –) and the numerical solution for the unknown boundary Γ_2, obtained with various levels of noise added into the displacement data $\boldsymbol{u}^{(\mathrm{an})}|_{\Gamma_1}$.

Figure 5 shows the iterative convergence process for the unknown boundary Γ_2 as the initial guess moves towards the target when obtained for $p = 1\%$ noise added into the displacement data $\widetilde{\boldsymbol{u}}|_{\Gamma_1}$, $\lambda = \lambda_{opt}$ according to the L-curve criterion and various numbers of iterations performed. It can be seen from this figure that the numerical results for the unknown boundary given by equation (43) are reasonable approximations of their exact value after a small number of iterations, e.g. $k = 20$ iterations. It should be noted that the final numerical results for the unknown boundary (43) are obtained after $k_{opt} = 39$ iterations.

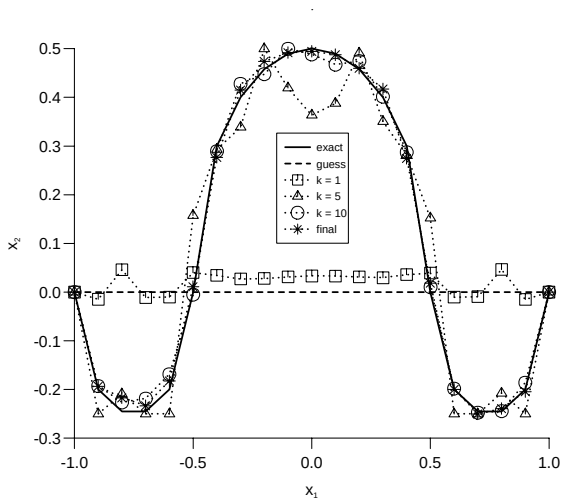

Figure 5: The iterative convergence process for the unknown boundary Γ_2 as the initial guess (– –) moves towards the target (——), obtained for $p = 1\%$ noise added into the displacement data $\boldsymbol{u}^{(\mathrm{an})}|_{\Gamma_1}$ and various numbers of iterations performed.

The importance of the choice of the optimal regularization parameter λ_{opt} is illustrated in Figure 6 which presents the exact values in comparison with the numerical solutions corresponding to different values of the regularization parameter, namely $\lambda < \lambda_{opt}$, $\lambda = \lambda_{opt}$ and $\lambda > \lambda_{opt}$, for the unknown boundary given by relation (43). From Figure 6, it can be seen that if the regularization parameter λ is taken to be too small then it produces oscillatory numerical solutions which are dominated by the contributions from the data errors, whilst if the regularization parameter λ is taken to be too large then it produces oversmooth numerical solutions which do not fit the given data, as discussed before.
Overall, from the numerical results presented in this section it can be concluded that the numerical method proposed for detecting an unknown part of the boundary of a solution domain occupied by an isotropic linear elastic medium produces a convergent and stable approximate solution with respect to decreasing the level of noise added into the input data.

References

[1] J. Hadamard, *Lectures on Cauchy Problem in Linear Partial Differential Equa-*

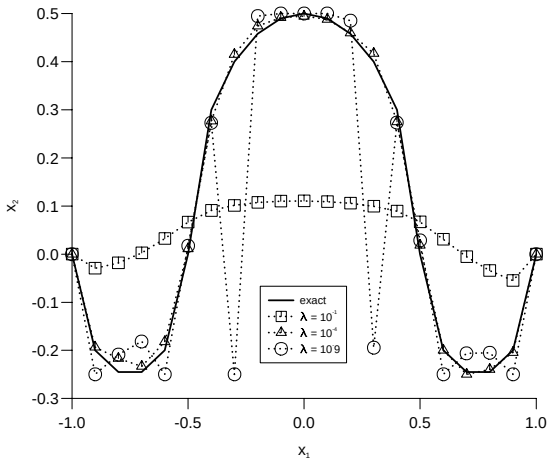

Figure 6: The exact (——) and the numerical solution for the unknown boundary Γ_2, obtained with $p = 1\%$ noise added into the displacement data $\boldsymbol{u}^{(\mathrm{an})}|_{\Gamma_1}$ and various values of the regularisation parameter λ, namely $\lambda < \lambda_{opt}$, $\lambda = \lambda_{opt}$ and $\lambda > \lambda_{opt}$.

tions. Yale University Press: New Haven, 1923.

[2] A.N. Tikhonov and V.Y. Arsenin, *Solutions of Ill-Posed Problems*. Winston-Wiley: Washington, 1977.

[3] M.A. Jaswon and G.T. Symm, *Integral Equation Methods in Potential Theory and Elastostatics*. Academic Press: London, 1977.

[4] G.T. Symm and R.A. Pitfield, Solution of Laplace's equation in two dimensions, *NPL Report NAC* **44**, 1974.

[5] A. Zeb, L. Elliott, D.B. Ingham and D. Lesnic, Solution of the Cauchy problem for Laplace equation. In: L. Elliott, D.B. Ingham and D. Lesnic (Eds.), *First UK Conference on Boundary Integral Methods* 1997: 297 – 307. Leeds, UK.

[6] S. Twomey, On the numerical solution of Fredholm integral equations of the first kind by the inversion of the linear system produced by quadrature, *J. Assoc. Comput. Mach.* 1963; **10**: 97 – 101.

[7] V.A. Morozov, On the solution of functional equations by the method of regularization, *Soviet Math. Dokl.* 1966; **7**: 414 – 417.

[8] G. Wahba, Practical approximate solution to linear operator equations when the data is noisy, *SIAM J. Numer. Anal.* 1977; **14**: 651 – 667.

[9] P.C. Hansen, Analysis of discrete and ill-posed problems by means of the L-curve, *SIAM Rev.* 1992; **34**: 561 – 580.

[10] L. Marin and D. Lesnic, BEM first-order regularisation method in linear elasticity for boundary determination, *Comput. Meth. Appl. Mech. Engng.* 2003; **192**: 2059 – 2071.

[11] O.D. Kellogg, *Foundations of Potential Theory*. New Haven: Dover, 1923.

[12] A.S. Saada, *Elasticity: Theory and Applications*. Pergamon Press: New York, 1974.

[13] C.A. Brebbia, J.F.C. Telles and L.C. Wrobel, *Boundary Element Techniques*. Springer-Verlag: Berlin, 1984.

[14] L. Marin, L. Elliott, D.B. Ingham and D. Lesnic, Boundary element method for the Cauchy problem in linear elasticity, *Engng. Anal. Boundary Elements* 2001; **25**: 783 – 793.

[15] P.E. Gill, W. Murray and M.H. Wright, *Practical Optimization*. Academic Press: London, 1981.

[16] S. Peneau, Y. Jarny and A. Sarda, Isotherm shape identification for a two-dimensional heat conduction problem. In: H.D. Bui, M. Tanaka, M. Bonnet, H. Maigre, E. Luzzato and M. Reynier (Eds.), *Inverse Problems in Engineering Mechanics* 1994: 47 – 53. Balkema, Rotterdam.

[17] D. Lesnic, J.R. Berger and P.A. Martin, A boundary element regularization method for the boundary determination in potential corrosion damage, *Inverse Probl. Engng.* 2002; **10**: 163 – 182.

[18] J.-M. Birginie, F. Allard and A.J. Kassab, Application of trigonometric boundary elements to heat and mass transfer problems. In: C.A. Brebbia, J.B. Martin, M.H. Aliabadi and N. Haie (Eds.), *BEM 18* 1996: 65 – 74. Braga, Portugal.

[19] P.C. Hansen, The L-curve and its use in the numerical treatment of inverse problems. In: P. Johnston (Ed.), *Computational Inverse Problems in Electrocardiology* 2001: 119 – 142. WIT Press, Southampton.